

## Article

# The Potential of Tufa as a Tool for Paleoenvironmental Research—A Study of Tufa from the Zrmanja River Canyon, Croatia

Jadranka Barešić <sup>1,\*</sup>, Sanja Faivre <sup>2</sup>, Andreja Sironić <sup>1</sup>, Damir Borković <sup>1</sup>, Ivanka Lovrenčić Mikelić <sup>1</sup>, Russel N. Drysdale <sup>3</sup> and Ines Krajcar Bronić <sup>1</sup>

- <sup>1</sup> Ruđer Bošković Institute, 10000 Zagreb, Croatia; asironic@irb.hr (A.S.); damir.borkovic@irb.hr (D.B.); ivanka.lovrencic@irb.hr (I.L.M.); krajcar@irb.hr (I.K.B.)  
<sup>2</sup> Department of Geography, Faculty of Science, University of Zagreb, 10000 Zagreb, Croatia; sfaivre@geog.pmf.hr  
<sup>3</sup> School of Geography, Earth and Atmospheric Sciences, University of Melbourne, Melbourne, Parkville, VIC 3010, Australia; rnd@unimelb.edu.au  
\* Correspondence: jbaresic@irb.hr

**Abstract:** Tufa is a fresh-water surface calcium carbonate deposit precipitated at or near ambient temperature, and commonly contains the remains of macro- and microphytes. Many Holocene tufas are found along the Zrmanja River, Dalmatian karst, Croatia. In this work we present radiocarbon dating results of older tufa that was found for the first time at the Zrmanja River near the Village of Sanaderi. Tufa outcrops were observed at different levels, between the river bed and up to 26 m above its present level. Radiocarbon dating of the carbonate fraction revealed ages from modern, at the river bed, up to 40 kBP ~20 m above its present level. These ages fit well with the hypothesis that the Zrmanja River had a previous surface connection with the Krka River, and changed its flow direction toward the Novigrad Sea approximately 40 kBP (Marine Isotope Stage 3). Radiocarbon AMS dating of tufa organic residue yielded a maximum conventional age of 17 kBP for the highest outcrop position indicating probable penetration of younger organic material to hollow tufa structures, as confirmed by radiocarbon analyses of humin extracted from the samples. Stable carbon isotope composition ( $\delta^{13}\text{C}$ ) of the carbonate fraction of  $(-10.4 \pm 0.6)\text{‰}$  and  $(-9.7 \pm 0.8)\text{‰}$  for the Holocene and the older samples, respectively, indicate the autochthonous origin of the carbonate. The  $\delta^{13}\text{C}$  values of  $(-30.5 \pm 0.3)\text{‰}$  and  $(-29.6 \pm 0.6)\text{‰}$  for organic residue, having ages <500 BP and >5000 BP, respectively, suggest a unique carbon source for photosynthesis, mainly atmospheric  $\text{CO}_2$ , with an indication of the Suess effect in  $\delta^{13}\text{C}$  during last centuries. The oxygen isotopic composition ( $\delta^{18}\text{O}$ ) agrees well with deposition of tufa samples in two stages, the Holocene  $(-8.02 \pm 0.72\text{‰})$  and “old” (mainly MIS 3 and the beginning of MIS 2)  $(-6.89 \pm 0.34\text{‰})$ , suggesting a  $\sim 4^\circ\text{C}$  lower temperature in MIS 3 compared to the current one.

**Keywords:** radiocarbon dating; carbonate and organic fraction; humin; C and O stable isotope composition; tufa; hard-water effect; Dinaric karst; Zrmanja river; Croatia; paleoenvironmental research



**Citation:** Barešić, J.; Faivre, S.; Sironić, A.; Borković, D.; Lovrenčić Mikelić, I.; Drysdale, R.N.; Krajcar Bronić, I. The Potential of Tufa as a Tool for Paleoenvironmental Research—A Study of Tufa from the Zrmanja River Canyon, Croatia. *Geosciences* **2021**, *11*, 376. <https://doi.org/10.3390/geosciences11090376>

Academic Editors: Bill Boyd and Jesus Martinez-Frias

Received: 12 July 2021

Accepted: 2 September 2021

Published: 7 September 2021

**Publisher's Note:** MDPI stays neutral with regard to jurisdictional claims in published maps and institutional affiliations.



**Copyright:** © 2021 by the authors. Licensee MDPI, Basel, Switzerland. This article is an open access article distributed under the terms and conditions of the Creative Commons Attribution (CC BY) license (<https://creativecommons.org/licenses/by/4.0/>).

## 1. Introduction

Tufa is a secondary carbonate wide spread within the karst areas worldwide. It is often the only available secondary carbonate within an area of important interest for paleoenvironmental investigation. Tufa precipitates from fresh waters (super)saturated in  $\text{CaCO}_3$  at ambient temperature and usually includes the remains of micro- and macrophytes, invertebrates, and bacteria [1–3]. Dating of tufa and its use as paleoenvironmental tool has always been connected with difficulties. Researchers have attempted to obtain reliable dates from tufa samples using various approaches, such as establishment of the direction

of tufa growth [4–8], radiocarbon dating after correction for the effects of “dead” carbon, or using U-Th dating. Additionally, tufa may erode, incorporate some allochthonous terrestrial material and “dead” carbonate, and experience recrystallization [9–11]. Reliable dating of tufa enables interpretation of the physico-chemical proxies and can provide many answers on Holocene and Pleistocene palaeoclimate [1,4,6,7,12–25]. It is essential that the results obtained by different analyses can be put into a correct time frame.

During tufa formation, a certain amount of “dead” carbon is incorporated (quantified as the “dead-carbon proportion”, or DCP). This dead carbon originates from carbonate in the source bedrock (limestones and dolomites) which does not contain  $^{14}\text{C}$ . Bedrock dissolution from  $\text{H}_2\text{CO}_3$  occurs due to the reaction of meteoric water with  $\text{CO}_2$  produced from plant degradation in soils. The  $\text{HCO}_3^-$  ions formed by this dissolution contains both  $^{14}\text{C}$ -dead bedrock carbon and modern or recent  $^{14}\text{C}$  from plants, lowering the initial radiocarbon activity ( $a_0$ ) of secondary carbonates precipitated from this water. Such waters emerging at springs are rich in  $\text{HCO}_3^-$  ions, and are characteristic of karst [26,27]. Measured radiocarbon dates appear older and must be corrected for DCP to obtain an accurate  $^{14}\text{C}$  age. The DCP can be determined since  $a_0$  can be obtained from radiocarbon activity of freshly sampled: (1) dissolved inorganic carbon (DIC); (2) carbonate precipitated on an inert material; or (3) actively precipitating tufa. The first method is the most reliable for reasons stated below. It is important to emphasize, however, that it is not known if the DCP established in this manner is constant through time, as is the case with the marine reservoir effect (MRE [28,29], and references therein, [30]), although the MRE and DCP have different origins. The DCP is often used in discussion of speleothem  $^{14}\text{C}$  ages [31–33]. However, in secondary carbonates, such as tufa and lake sediments of the Croatian karst, DCP in precipitated carbonate may be higher due to the incorporation of weathered limestone fragments into the precipitate [34]. For these reasons, herein we will use terms “hard-water effect” or “fresh-water effect” rather than the DCP.

U-Th dating is an alternative to radiocarbon dating although it is not free of inherent limitations. It can be applied if a tufa sample is compact, hard, and/or crystalline [11,32]. If tufa is not compact, dating can be obtained by tufa leachate isochron method [12,35–37], but this technique does not necessarily solve the dating problem [38]. Recent work suggests many U-Th tufa dates are rejected and dating of both the carbonate fraction and organic residue from tufa by the radiocarbon method is the most reliable method [6–8], in spite of the difficulties with this latter approach [39]. It has been suggested that the only possibility of accurately dating secondary so-called “dirty” carbonates, such as tufas, is radiocarbon dating of the organic residue of the sample, since this part should not be influenced by erosion and recrystallization as is the case with the carbonate fraction [8]. Humic is generally regarded as the most resistant organic component and the best representative of true age, and is often used in geochronology [40–44].

Consequently, in this study radiocarbon dating of both carbonate and organic fractions has been implemented, as well as the stable isotopic composition of carbon (carbonate and organic fractions, extracted humin) and oxygen (carbonate fraction), in order to investigate the chronology of Zrmanja River Canyon development (Croatia, Dalmatian karst). Chronology will be discussed on the basis of 12 tufa samples found over a range of elevations from the river bed to 26 m above the stream level.

## 2. Materials and Methods

### 2.1. Site Description

The Zrmanja River is a relatively small river in Dinaric karst, Dalmatia, Croatia (Figure 1) with a total length of 72.5 km [45]. It receives water from many smaller springs and creeks on its route. The biggest contribution comes from the Krupa River, whose confluence with the Zrmanja River occurs 47 km from the spring of Zrmanja, downstream of Sanaderi. Similar to many rivers in the Croatian karst (e.g., Cetina [46]) according to its geomorphological properties the Zrmanja has a composite river valley characterized by an interchange of carbonate canyons and zones of lateral valley widening. The canyons are of

~20 m depth with variable widths. Generally, canyon slopes are rocky with poor vegetation (typically Mediterranean type), and at the Sanaderi location the tufa is partially concealed by grasses and trees.

The Zrmanja River changes its flow direction between the Palanka and the Sanaderi villages (Kravlja Draga) and turns from N-S to an almost E-W direction (Figure 1c). This is where the Zrmanja River may have had a surface connection with the Krka River (approximately 40 kyears ago [47]). The fossil river bed can be discerned in places while the groundwater connection with the Krka River has been shown from dye-tracing experiments performed during 1980s [48,49].

**Table 1.** Geographical coordinates, approximate elevations, and height above the water level of samples at the Sanaderi location (Figure 1). Comments regarding microlocations and sample description are also given.

Sample No.	Geographical Coordinates	Elevation (m asl)	Height above Water Level (m)	Comment	Description
1		52	0	Approximately at 1 m horizontal distance from river bed	Porous, moss remains and soil incorporated, very hard, white—light yellow, not laminated, not clear if autochthonous or not
2	N 44°08'57" E 15°53'13"	54	2	4 m horizontal distance from river bed	Porous, soil incorporated with lots of moss, very soft, reddish, not laminated
3		52	0	1 m horizontal distance from river bed	Porous, soil incorporated with moss, very soft, reddish, not laminated
4		53	1	Exactly below sample 2	Porous, hard, slightly laminated with moss overgrowth, grey—yellowish
5	N 44°09'02" E 15°53'12"	72	20	Approximately 50 m horizontal distance from Zrmanja R.	Nicely laminated, non-porous, brown and yellow laminae, moderately hard, compact
6		73	21	Outcrop along the road, approximately 50 m horizontal distance from Zrmanja R.	Laminated, medium porosity, white and yellowish laminae, soft
7		72	20	1 m below sample #6, The same outcrop as #6	
8	N 44°09'06" E 15°53'08"	73	21	1 m horizontal distance from sample #6, from the same outcrop	Nicely laminated, non-porous, brown and yellow laminae, moderately hard, compact
9		72	20	1 m horizontal distance from sample #7 at the same height (approx. 20 m above water level) and 1 m below the sample #8 of the same outcrop along the road as #6	Laminated, medium porosity, white and yellowish laminae, soft
10	N 44°09'06" E 15°53'10"	69	17	Approximately 25 m horizontal distance from Zrmanja R. Below outcrop with samples #6–9	Non-porous, no visible remains of plants and soil, white-yellowish, laminated
11	N 44°09'06" E 15°53'07"	77	25	Outcrop approximately 100 m horizontal distance from Zrmanja R., bottom of outcrop	Porous, no visible remains of plants and soil, white-yellowish, soft
12		78	26	Top of the same outcrop as #11	Non-porous, no visible remains of plants and soil, white-yellowish, laminated, soft

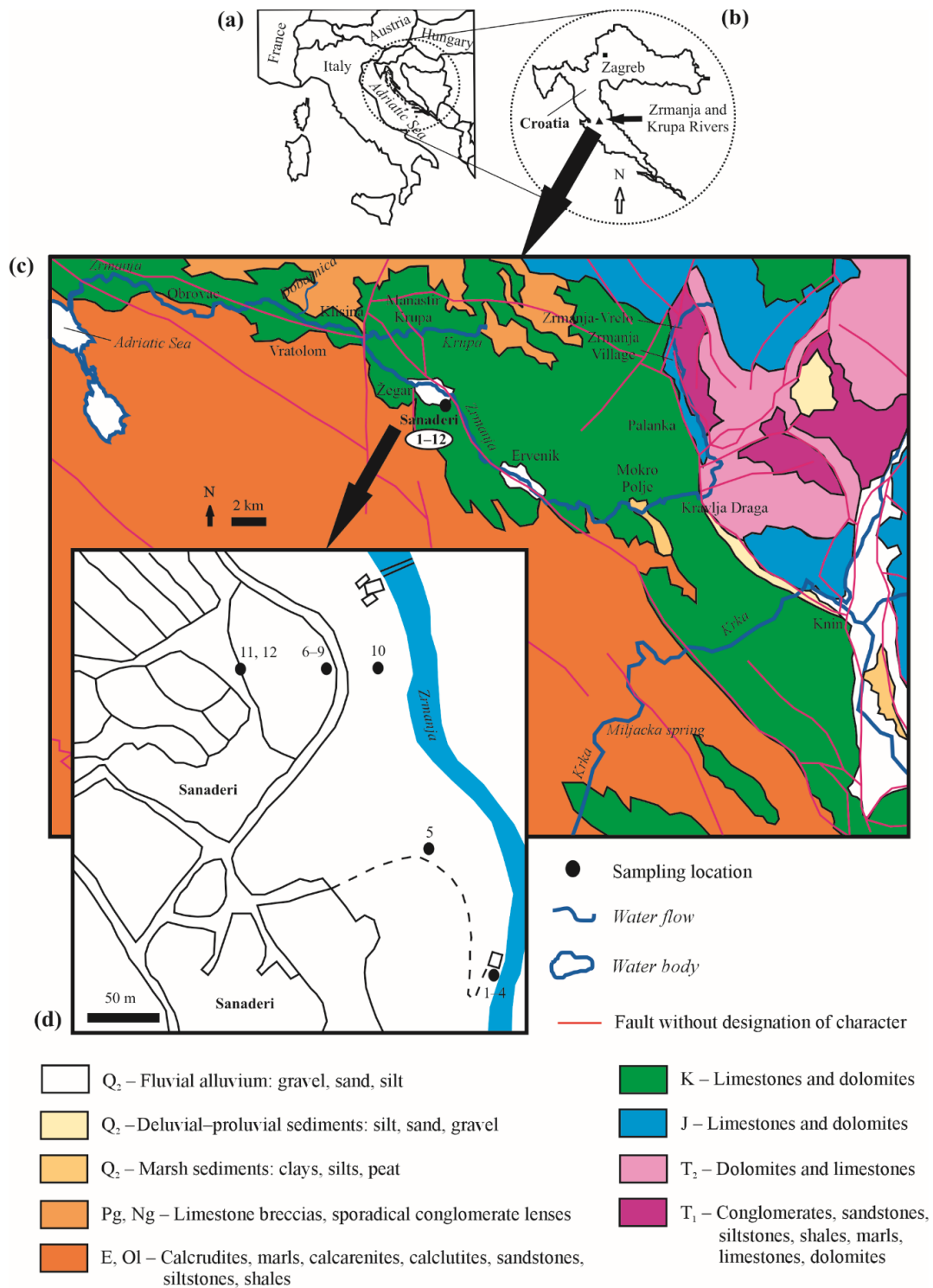


**Figure 1.** (a) Geographical position of Croatia within Europe; (b) position of the investigated area within Croatia; (c) geological map of investigated area [50]; for full understanding of this study, Kravlja Draga, where the Zrmanja River changes its course, is also presented as well as the Krka River and Miljacka Spring; (d) enlarged area of the Sanaderi location, black dots ● mark sampling locations, and the numbers represent tufa sample numbers, see Table 1 for details.

### 2.2. Sampling

Four tufa samples were collected at the Zrmanja river bed and eight fossil tufa samples were collected at the higher levels of Zrmanja River Canyon near Sanaderi (Figure 1) during sampling in 2015. Fluvial tufa samples were collected along the course of the river (samples

#1–4), up to 2 m above water level (Table 1, Figure 1). Fossil tufa samples (#5–12) were collected at different levels above the river-bed (17–26 m) (Table 1, Figure 1) found on Cretaceous limestones and dolomites. Approximately 1 kg per sample was taken at each site, placed into a labelled plastic bag and transported to the laboratory.

Tufa samples from the investigated locations differ in color and morphology (Table 1, Figure S1). The majority can be classified as encrusted mossy deposits, except for samples #5–8, which can be classified as algal laminated crusts [51].

### 2.3. Measurement Methods

Specific radiocarbon activity  $a^{14}\text{C}$  in carbonate samples/fractions was determined by the liquid scintillation technique (LSC). Between 50 and 70 g of sample was dissolved in HCl (18%) in an inert  $\text{N}_2$  atmosphere and the obtained  $\text{CO}_2$  was converted to  $\text{C}_6\text{H}_6$  in a vacuum synthesis line. Benzene samples were measured on an LSC Quantulus 1220 [52,53].

The bulk residue after the carbonate dissolution was neutralized, dried, and prepared as graphite for  $a^{14}\text{C}$  AMS measurements; herein it is referred to as the organic fraction. About 10–15 mg of each residue sample was combusted in pre-evacuated sealed quartz tube (850 °C). The humin samples were obtained from the bulk residue of the organic fraction by acid-alkali-acid method [54–56] and combusted in sealed quartz tubes. The obtained  $\text{CO}_2$  was converted to graphite by Zn reduction [54]. Graphite samples were pressed into aluminum holders and sent to the accelerator mass spectrometry (AMS) facility at the Centre for Applied Isotope Studies (CAIS), University of Georgia, USA. An aliquot of  $\text{CO}_2$  obtained from organic tufa residue combustion was vacuum sealed in a glass tube and sent to the same laboratory for  $\delta^{13}\text{C}$  determination. Graphite samples were measured by 0.5 MeV accelerator mass spectrometer (AMS) and  $\delta^{13}\text{C}$  was measured by isotope ratio mass spectrometer (IRMS) [57].

For both LSC and AMS techniques, Oxalic Acid II (SRM NIST4990C) was used as the primary reference material, and anthracite and Carrara marble as the background materials. As a control sample (a sample of well-defined  $a^{14}\text{C}$  prepared as an unknown sample), humic acid T ( $a^{14}\text{C} = 65.82$  pMC) from the VIRI intercomparison [54] exercise and ANU sucrose ( $a^{14}\text{C} = 150.6$  pMC) were used for the AMS and LSC techniques, respectively.

Results of the radiocarbon measurements, normalized by  $\delta^{13}\text{C}$  to  $-25\text{‰}$ , are expressed as relative specific activity  $a^{14}\text{C}$  (in units pMC, percent Modern Carbon) and as a conventional radiocarbon age (expressed in year Before Present, BP, where 0 BP = 1950 AD). Calibrated ages (cal BP) were obtained using OxCal software [58,59] and the IntCal20 calibration curve with included respective initial activities (hard-water corrections) for carbonate and organic fractions [60]. Correction for the hard-water effect is reported here either as initial activity  $a_0$  or/and reservoir age defined as:

$$R = -8033 \times \ln a_0. \quad (1)$$

Stable oxygen and carbon isotope values ( $\delta^{18}\text{O}$  and  $\delta^{13}\text{C}$ ) of carbonates were measured at the University of Melbourne, Australia using an AP2003 continuous flow mass spectrometer. Approximately 0.8 mg of carbonate sample was analyzed [61], with analytical uncertainties better than 0.10‰ for  $\delta^{18}\text{O}$  and 0.05‰ for  $\delta^{13}\text{C}$ .

### 3. Results

Results of radiocarbon dating and stable isotope compositions of tufa carbonate fraction of 12 samples from the Sanaderi location are shown in Table 2. Samples adjacent to modern river level (0–2 m) gave Holocene ages, while samples from tufa outcrops from the upper parts (elevations 17–26 m above the water level) gave radiocarbon conventional ages above 22,000 BP.  $\delta^{13}\text{C}$  values of the carbonate component range from  $-10.4\text{‰}$  to  $-8.5\text{‰}$ , while  $\delta^{18}\text{O}$  values range from  $-7.4\text{‰}$  to  $-6.4\text{‰}$ .

**Table 2.** Results of isotopic analyses of tufa samples,  $a^{14}\text{C}$ ,  $\delta^{13}\text{C}$  and  $\delta^{18}\text{O}$  in carbonate fraction. Sample numbers defined in Table 1 and Figure 1.

Sample No.	Height above Water Level (m)	Lab. No. Z-xxxx	$a^{14}\text{C}$ (pMC)	Conventional Age (BP)	$\delta^{13}\text{C}$ (‰)	$\delta^{18}\text{O}$ (‰)
1	0	5951	40.35 ± 0.23	7290 ± 45	−8.96	−7.40
2	2	5952	89.5 ± 1.0	890 ± 95	-	-
3	0	5953	83.11 ± 0.55	1485 ± 55	−9.13	−7.42
4	1	5954	77.61 ± 0.60	2035 ± 60	-	-
5	20	5955	2.69 ± 0.12	29,040 ± 360	−9.85	−7.01
6	21	5956	0.78 ± 0.12	39,000 ± 1250	−10.33	−7.19
7	20	5957	5.29 ± 0.15	23,600 ± 230	−9.94	−7.25
8	21	5958	1.05 ± 0.13	36,600 ± 1000	−10.5	-
9	20	5959	2.03 ± 0.12	31,300 ± 480	-	-
10	17	5960	4.06 ± 0.14	25,740 ± 280	−8.47	−7.04
11	25	6295	0.81 ± 0.13	38,700 ± 1300	−10.39	−6.35
12	26	6296	6.46 ± 0.16	22,000 ± 200	−8.64	−6.49

Results of radiocarbon dating of tufa organic fraction of samples from the Sanaderi location (except sample #9), shown in Table 3, yielded the Holocene dates for seven out of eleven samples. The organic residue of the sample #6 (12,060 ± 30 BP) was significantly older than sample #8 (7365 ± 30 BP) and corresponds to the end of the last glaciation, although it was sampled from approximately the same layer of the same tufa outcrop. Two samples from higher elevations, samples #11 and #12, were dated to 17,000 ± 40 BP and 15,980 ± 35 BP, respectively, i.e., within the glacial period. Four samples were selected for humin dating. The humin was extracted from samples #3 (Holocene), #6, #7, and #11 (older than the Holocene period, later referred as “old”). Two results from the humin component, compared to organic residue, gave slightly lower  $a^{14}\text{C}$  values: the sample #3 and #7 for approximately 1.2 pMC and 2.2 pMC, respectively (Table 3). The humin extracted from samples #6 and #11, compared to organic residue, yielded higher  $a^{14}\text{C}$  values for 19.6 pMC and 11.2 pMC, respectively (Table 3).

**Table 3.**  $a^{14}\text{C}$ , radiocarbon dates and  $\delta^{13}\text{C}$  values of the organic residues and the humin of tufa samples from the Sanaderi location.

Sample No.	Lab. No. Z-xxxx	$a^{14}\text{C}$ (pMC)	Conventional Age (BP)	$\delta^{13}\text{C}$ (‰)
1	6458	51.8 ± 0.2	5285 ± 25	−29.96
2	6630	99.7 ± 0.3	25 ± 20	−30.85
3	6454	95.5 ± 0.3	370 ± 20	−30.27
3	7608, humin	94.3 ± 0.3	470 ± 20	−30.26
4	6631	95.7 ± 0.3	355 ± 20	−30.39
5	6455	26.7 ± 0.1	10,600 ± 30	−28.92
6	6459	22.3 ± 0.1	12,060 ± 30	−29.52
6	7610, humin	41.9 ± 0.2	6995 ± 45	−28.60
7	6460	29.3 ± 0.1	9870 ± 25	−28.80
7	7611, humin	27.1 ± 0.1	10,500 ± 30	−28.80
8	6461	40.0 ± 0.1	7365 ± 30	−29.38
10	6462	34.2 ± 0.1	8630 ± 30	−29.59
11	6456	12.1 ± 0.1	17,000 ± 40	−29.84
11	7609, humin	23.3 ± 0.1	11,700 ± 35	−29.93
12	6457	13.7 ± 0.1	15,980 ± 35	−30.70

## 4. Discussion

### 4.1. Isotope Analyses of Carbonate and Tufa Ages

The obtained conventional ages of secondary carbonates in karst areas usually appear older than true due to the hard-water effect, i.e., reservoir  $^{14}\text{C}$  age. In such cases, the initial

radiocarbon activity,  $a_0$ , should be determined [26]. In this work  $a_0$  was determined from the  $a^{14}\text{C}$  of dissolved inorganic carbon (DIC) in water from which tufa precipitates, giving the most reliable information among the possibilities described earlier. For the Sanaderi location,  $a^{14}\text{C}$  of DIC was  $84.5 \pm 0.3$  pMC resulting in reservoir age of  $1350 \pm 20$  years [62].

The mean values of  $\delta^{13}\text{C}$  of tufa carbonates ( $-9.6 \pm 0.8\text{‰}$ , Table 2) and  $\delta^{13}\text{C}$  of DIC ( $-11.4\text{‰}$  [62]) indicate authigenic precipitation of carbonates from DIC. Both values are similar to the mean values of DIC and authigenic carbonate from another Dinaric karst system, Plitvice Lakes ( $-10.9 \pm 1.3\text{‰}$  and  $-8.9 \pm 1.1\text{‰}$ , respectively) [34,63]. At the same time there is practically no difference in  $\delta^{13}\text{C}$  values between the Holocene (mean value  $-10.04 \pm 0.57\text{‰}$ ,  $n = 18$ ) and older samples (“old”) (mean value  $-9.73 \pm 0.78\text{‰}$ ,  $n = 6$ ) (Figure 2a). Here, the Holocene  $\delta^{13}\text{C}$  value data for the Zrmanja River tufa samples were taken from [64]. These values indicate that during the tufa deposition carbon source did not change. There is also no indication of a change in the hard-water effect in the past and we may assume that the  $a^{14}\text{C}$  of DIC ( $84.5 \pm 0.3$  pMC) presents the initial activity for all tufa samples (Table 4).

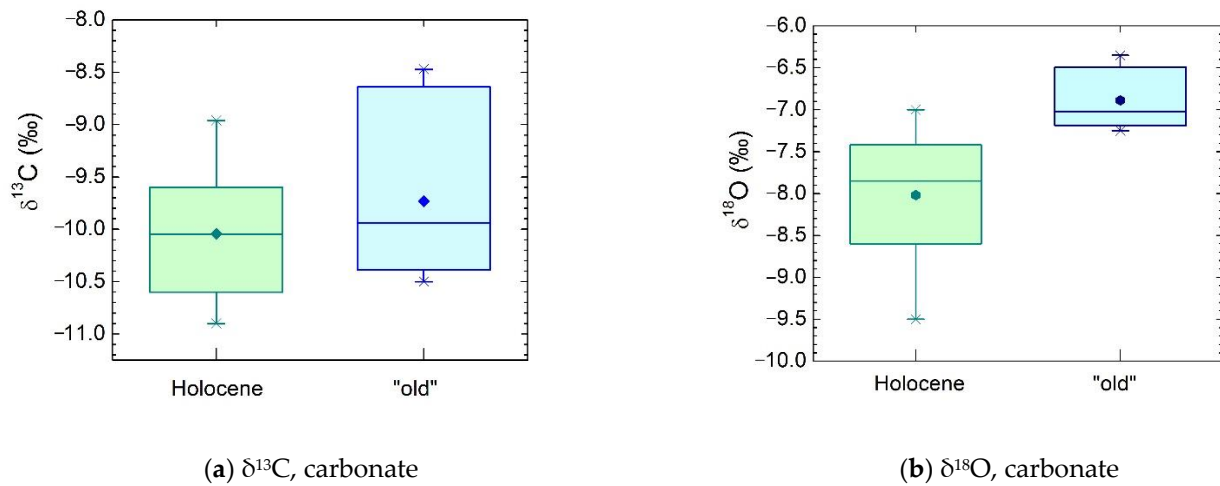


**Figure 2.** Box-plot of (a)  $\delta^{13}\text{C}$  and (b)  $\delta^{18}\text{O}$  values for Holocene and “old” samples. Data for the Holocene tufa samples taken from Table 2 and [64].

**Table 4.** The  $a^{14}\text{C}$  difference between organic/humin and carbonate fractions,  $^{14}\text{C}$  reservoir corrected calibrated ages of tufa carbonate fractions from the Sanaderi location ( $a_0 = 84.5 \pm 0.3$  pMC,  $R = 1350 \pm 20$  years), and calibrated ages of organic residues ( $a_0 = 97.0 \pm 0.9$  pMC,  $R = 240 \pm 70$  years).

Sample No.	$a^{14}\text{C}$ Difference (pMC)	Carbonate Fraction		Organic Residue and Humic	
		Calibrated Age Span (cal BP) (68.3%)	Calibrated Age Median (cal BP)	Calibrated Age Span (cal BP) (68.3%)	Calibrated Age Median (cal BP)
1	11.45	6988–6874	6931	5869–5765	5811
2	10.2	1956–1957 cal AD (14.6%)	2007 cal AD	1956–1956 cal AD	1956 cal AD
		2006–now cal AD (53.6%)			
3 3 humin	12.39	275–160	218	196–104	148
	11.2			283–209	245
4	18.09	842–696	770	180–84	131
5	25.01	32,534–31,579	32,060	12,411–12,291	12,344
6 6 humin	21.52	42,417–40,780	41,684	13,770–13,656	13,714
	41.1			7631–7526	7578

Table 4. Cont.

Sample No.	$a^{14}\text{C}$ Difference (pMC)	Carbonate Fraction		Organic Residue and Humin	
		Calibrated Age Span (cal BP) (68.3%)	Calibrated Age Median (cal BP)	Calibrated Age Span (cal BP) (68.3%)	Calibrated Age Median (cal BP)
7 7 humin	24.01	26,821–26,349	26,582	11,131–11,052	11,089
	22.3			12,277–12,102	12,188
8	38.95	40,791–39,291	40,042	7972–7884	7928
9	-	34,958–33,994	34,491	-	-
10	30.14	28,976–28,400	28,689	9449–9358	9397
11 11 humin	11.3	42,277–40,558	41,501	20,366–20,225	20,294
	22.5			13,373–13,270	13,320
12	7.24	25,220–24,786	25,003	19,100–18,958	19,031

The dating results of samples from higher positions at Sanaderi, samples #5–12 (Tables 1 and 2), imply that tufa grew during Marine Isotope Stage 3 (MIS 3) and the beginning of MIS 2, a finding not previously found in Croatia. This would also mean that the Zrmanja River bed was approximately 20 m higher some 40 kyears ago compared to its current position. Furthermore, this is in accordance with the assumption that the Zrmanja River changed its watercourse approximately 40 kyears ago [47].

#### 4.2. Possibility of Tufa Isotopic Composition of Oxygen as Paleoclimate Proxy

The oxygen isotopic composition of tufa samples analyzed within this work ranges from  $-7.4\text{‰}$  to  $-6.4\text{‰}$  (Table 2). Similar  $\delta^{18}\text{O}$  values of tufa from interglacial have been found in other regions of the Dinaric karst [2–4]. This indicates that all tufa samples from this work precipitated during warm periods. Considering the  $\delta^{18}\text{O}$  values,  $^{14}\text{C}$  dates of carbonate fractions are assumed correct, even for samples of ages close to the radiocarbon detection limit. Other indications of the relevant dates of the samples can be obtained from the difference of  $\delta^{18}\text{O}$  values between the Holocene samples (younger than 10,000 BP (11,700 cal BP)) and the “old” samples (older than 20,000 BP), Figure 2b. The Holocene samples, which have a mean value of  $\delta^{18}\text{O} = -8.02 \pm 0.72\text{‰}$  ( $n = 18$ , present data and data from [64]), precipitated from water of approximate temperature of  $16.4\text{ °C}$  calculated from paleotemperature Equation (2) [65]:

$$T\text{ (°C)} = 15.7 - 4.36 \times (\delta_c - \delta_w) + 0.12 \times (\delta_c - \delta_w)^2, \quad (2)$$

where  $\delta_c$  is  $\delta^{18}\text{O}$  mean value vs. VPDB for either the Holocene or old carbonate samples, and  $\delta_w$  is  $\delta^{18}\text{O}$  mean value vs. VSMOW of water from Miljacka Spring,  $-7.8\text{‰}$  (Figure 1c).

Water temperature and  $\delta^{18}\text{O}$  data were obtained from one of the Krka River Springs, Miljacka Spring [66,67], which is completely fed by Zrmanja water [68,69]. The temperature range of Miljacka water obtained by 2-year seasonal measurement [66] was  $8.8\text{--}14.5\text{ °C}$  so we may assume that Equation (2) [65] is applicable here. The difference between calculated and measured temperature values is expected since tufa precipitates more intensively during spring and summer [4] and due to cooling of Zrmanja water through the underground flow. The mean value of  $\delta^{18}\text{O} = -6.89 \pm 0.34\text{‰}$  ( $n = 6$ ) for the “old” samples indicates their precipitation at approximate water temperature of  $12.5\text{ °C}$ . The temperature difference of  $\approx 4\text{ °C}$  between the Holocene and “old” tufa calculated here is similar to the temperature difference between the Holocene and MIS 3 presented in [70–72]. This further means that “old” tufa could have precipitated during MIS 3 and beginning of MIS 2.

The Holocene  $\delta^{18}\text{O}$  values obtained from the Zrmanja area (present results and data from [64]) are higher (between  $-9.5\text{‰}$  and  $-7.0\text{‰}$ ) than the Holocene authigenic carbonates from a well investigated area of the Plitvice Lakes system, where  $\delta^{18}\text{O}$  ranges between  $-11.9\text{‰}$  and  $-8.7\text{‰}$  [2–4,34,64,73]. This can be explained by environmental settings, and

continental and altitude effects [4,64,74–78]. The Plitvice Lakes are at higher elevations (between 400 and 700 m asl) and are characterized by the moderate mountain climate (Cfb) compared to the Zrmanja locations with Csa climate type [79–81] and at lower elevations (<100 m asl). The Holocene tufa from the Krka River have  $\delta^{18}\text{O}$  values in the same range as tufa from Zrmanja (from  $-8.5\text{‰}$  to  $-7.8\text{‰}$ ) since both locations are situated within the same geographic area [4,66,67].

#### 4.3. Tufa Age Implications from Isotope Analyses of Organic Residues and Extracted Humic

$^{14}\text{C}$  analyses of tufa organic residues gave higher  $a^{14}\text{C}$  values compared to that of the carbonate fractions (Tables 2–4). The difference is expected due to a different intensity of the hard-water effect in organic and carbonate fractions [6,39,62,63]. In order to accept the obtained dates as reliable, the difference in  $a^{14}\text{C}$  values between the organic residue and the carbonate should not be larger than 15 pMC [39,82]. However, recent authigenic and consolidated sediments from the Plitvice Lakes showed that the  $a^{14}\text{C}$  differences between carbonate and organic fractions could be up to 20 pMC [63,83] and we consider the value of 20 pMC as a criterion for acceptable results. Six out of 11 samples have differences of  $a^{14}\text{C}$  between organic residue (humic is not regarded here) and carbonate fraction of less than 20 pMC (Table 4).

The hard-water effect is also observed in organic matter since it is a mixture of different organics that photosynthesize from DIC and atmospheric  $\text{CO}_2$  [26,62,84–86]. Age correction due to a hard-water effect for organic matter is usually lower than that in the carbonate fraction [26]. The  $\delta^{13}\text{C}$  values of organic residue in analyzed tufa samples are within the narrow range between  $-30.85\text{‰}$  and  $-28.6\text{‰}$  (Table 3) which indicates mainly constant origin of carbon in organic matter, namely that of atmospheric  $\text{CO}_2$ .

The hard-water effect of the organic matter was determined from  $a^{14}\text{C}$  of the fresh moss sample, *Eucladium verticillatum*. The  $\delta^{13}\text{C}$  value of  $-34.2\text{‰}$  and  $a^{14}\text{C}$  value of  $97.0 \pm 0.9$  pMC (Z-5948) of this moss indicate that atmospheric  $\text{CO}_2$  is the main source of carbon with a possibility of incorporating DIC if flooded [62]. Additionally, the Suess effect [87], i.e., lower  $\delta^{13}\text{C}$  values of atmospheric  $\text{CO}_2$  today than in the past, may also contribute to lower  $\delta^{13}\text{C}$  of moss. The Suess effect is confirmed by the clear difference between  $\delta^{13}\text{C}$  values for recent samples (<500 years:  $-30.5 \pm 0.3\text{‰}$ ,  $n = 3$ ) and older samples ( $-29.6 \pm 0.6\text{‰}$ ,  $n = 8$ ), as shown in Figure 3. There is also no difference between the Holocene (5–10 kyears:  $\delta^{13}\text{C} = -29.4 \pm 0.4\text{‰}$ ,  $n = 4$ ) and the “old” samples (>10 kyears:  $-29.8 \pm 0.6\text{‰}$ ,  $n = 4$ ). These results imply that the carbon source of organic residue has been constant in the past. Since the  $a^{14}\text{C}$  of atmospheric  $\text{CO}_2$  today is almost equal to 100 pMC [88–90]  $a_0$  for organic residue is set as 97 pMC (reservoir age of  $240 \pm 70$  years) for age calculation for all organic residue samples (Table 4). Because of the small value of the reservoir age for organic residue, the ages of dated samples did not change significantly (Table 4). As a consequence, the difference between corrected and calibrated carbonate and organic fraction ages diminished for the Holocene tufa (Table 4) and a good correlation between calibrated dates is obtained (Pearson’s  $r = 0.99$ , Figure 4a). On the contrary, there is no correlation between the ages of the carbonate and organic fraction in older samples ( $r = 0.05$ , Figure 4b). The absence of a correlation for the “old” samples (Figure 4b) and the large difference in  $a^{14}\text{C}$  values of organic and carbonate fractions (Table 4) indicate that there should be an additional source of these effects. The ages of the organic fractions are especially suspicious since they suggest that tufa was mainly deposited during the MIS 2 cold period, [91–94] which is generally regarded as unfavorable for tufa precipitation [4,95].

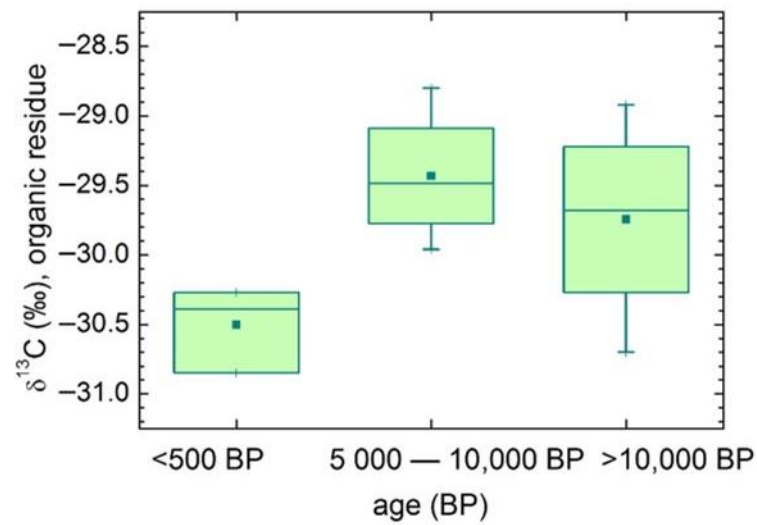


Figure 3.  $\delta^{13}\text{C}$  values of tufa organic residues for different groups of ages.

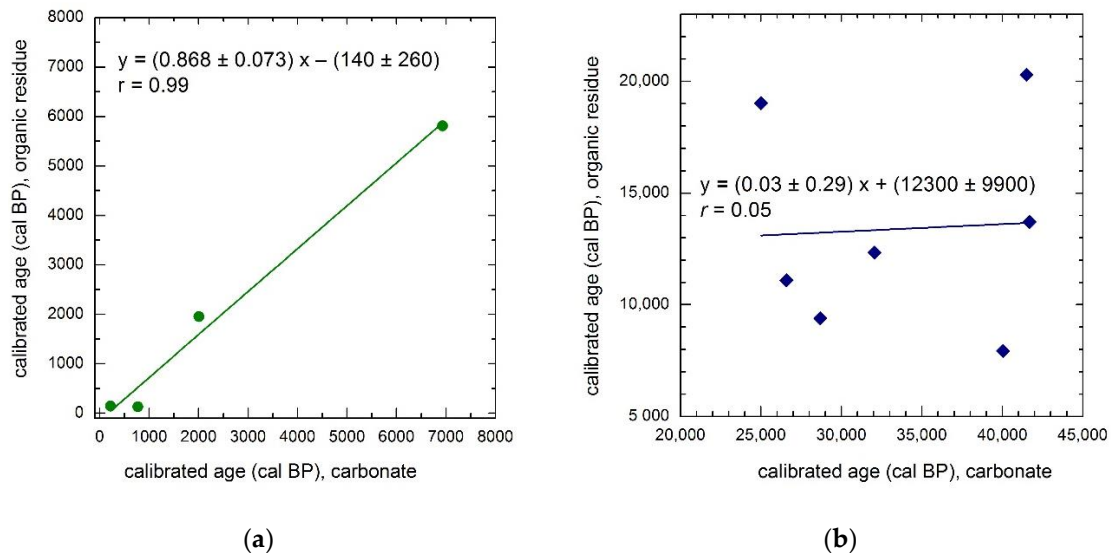


Figure 4. Calibrated ages of the organic residue vs. calibrated ages of the carbonate component of the tufa samples from Sanaderi. (a) the Holocene samples; (b) the “old” samples.

A plausible explanation can be proposed after considering the humin analyses. The humin fractions extracted from samples #3 and #7 have almost the same values of  $a^{14}\text{C}$  as the bulk organic residue (1.2 and 2.2 pMC difference, respectively) and their  $\delta^{13}\text{C}$  values were equal to those of the bulk organic measurements (Table 3). Humin extracted from samples #6 and #11 yielded higher  $a^{14}\text{C}$  values for 19.6 and 11.2 pMC, respectively (Table 3). The differences in radiocarbon ages between the bulk organic residue and the humin component are probably due to the penetration of roots and plants through porous tufa after its deposition [38,39]. The sample #6 has the biggest difference between its humin and organic fraction (19.6 pMC), and it is the only sample with a significant difference in  $\delta^{13}\text{C}$  values of 0.9‰ (Table 3). Such a difference in  $\delta^{13}\text{C}$  can be expected if the Suess effect is considered (Figure 3) and this would indicate that very recent plants penetrated an old tufa deposit, shifting the organic  $a^{14}\text{C}$  in the direction of a younger age for the tufa.

#### 4.4. The Zrmanja River Canyon Development

Radiocarbon ages obtained on the different fractions (carbonate, organic) give two possible scenarios of tufa deposition and, consequently, Zrmanja River Canyon devel-

opment. All radiocarbon data of tufa found just above the water level (samples #1–4) confirm tufa deposited during the Holocene (Figure 5). Data obtained from samples #5–12, found at elevations between 17 and 26 m above the present water level, differ significantly. Carbonate fraction dates suggest deposition of higher tufa samples during MIS 3 and the beginning of MIS 2 and formation of the canyon principally after MIS 3 (Figure 5). Organic residue results offer an alternative of canyon development in MIS 2 and the Holocene (Figure 5). In both cases, two groups are clearly distinguished: recent samples positioned just above the river bed, and older samples positioned at levels approximately 20 m above the river bed.

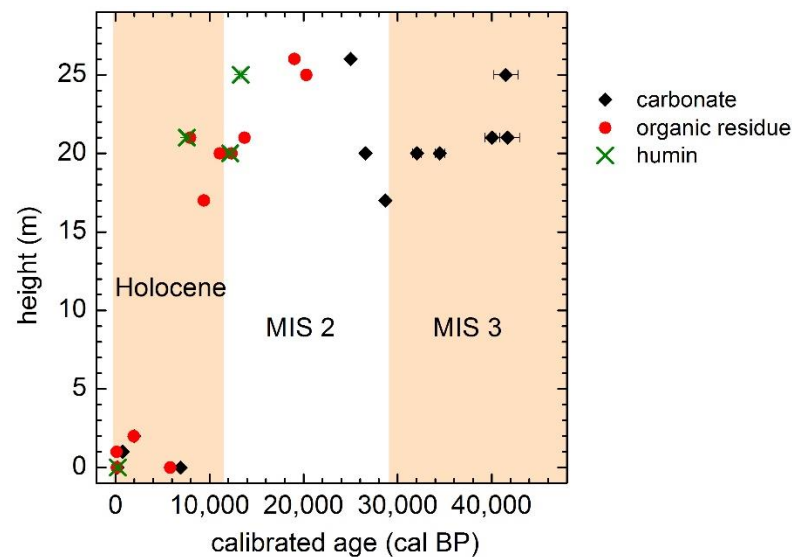


**Figure 5.** Positions of tufa above river bed vs. calibrated ages of Sanaderi samples: carbonate ages are corrected for hard-water effect of 1350 years and organic and humin for 240 years.

In the External Dinarides, the Last Glacial Maximum (LGM) was characterized by a cold climate, as indicated by numerous glacial morphological features, e.g., at the nearby Velebit Mt. found above 800–900 m asl [96–99] where average annual temperature was estimated to be 10 °C lower than today. Local conditions enable the formation of large snow packs and regional glaciations with estimated ice thickness of around 200 m [97]. Tufa formation is not expected in such cold-climate conditions. However, along the eastern Adriatic coast, growth of speleothems is recorded during the LGM [100–102]. During the LGM, conventionally 21 kBP, sea level was at its lowest at  $-121 \pm 5$  m below present [103]. Thus, a significant part of the Adriatic Sea area was dry land [100,104]. However, since that period the relative sea level (RSL) started to rise, so a change in fluvial system is expected, from incision toward deposition. Consequently, the incision of ~20 m between 8 kyears and 6 kyears as suggested using  $^{14}\text{C}$  dating of organic residue and humin (Figure 5) is unlikely.

During MIS 3, the RSL generally dropped [100,105,106]. Due to the erosional base level lowering, river valleys were generally getting longer, inducing the dominant trend of vertical erosion in the valleys. However, periods of RSL stability in the second part of MIS 3 [107,108] could have favored tufa formation. The further, rapid sea level lowering during early MIS 2 would have supported active fluvial incision processes.

Furthermore, the accumulation of tufa deposits in Mediterranean regions seems to start generally at the end of MIS 2 or at the MIS 2—MIS 1 transition, i.e., after 14 kyears in Spain ([109] and reference therein) and after 13 kyears on different locations in France ([110] and reference therein). Tufa deposition episodes during  $32 \pm 10$  kyears were also defined on several locations in Spain [110]. Accordingly, we strongly support the period of tufa deposition at Sanaderi location principally during MIS 3.

Consequently, the two episodes of tufa formation during MIS 3 to beginning of MIS 2 and during MIS 1 (Middle and Late Holocene) reflect fluvial system response driven

predominantly by climate change and RSL change. So, we assumed, as generally accepted, that tufa deposits formed during temperate/warm interglacial periods and interstadials (e.g., [109]), while downcutting occurred under rather colder conditions, i.e., at Sanaderi location, roughly between 25,000 and 6000 cal BP with the mean incision rate of around 1.1 mm/yr. However, incision could have also started earlier. All obtained results are close to the conclusions of earlier work of Fritz [47], who defined the main downcutting period in a single phase that lasted from 40,000 to 8500 BP.

## 5. Conclusions

Isotope analyses of tufa from the Zrmanja River near Sanaderi, Dalmatia, Croatia, are presented. For the first time, tufa from a period pre-dating the Holocene, was found in the Zrmanja River area and this is the first time that tufa from MIS 3 and the beginning of MIS 2 has been found in Croatia. The carbon stable isotope composition of the carbonate fraction indicates that tufa formation in all periods was authigenic, without incorporation of old detrital limestone and therefore suitable for paleoenvironmental research. Radiocarbon dating of tufa samples found at the river-bed level revealed similar ages of both organic and carbonate fractions (the Holocene). Radiocarbon ages of tufa samples found at higher positions (~20 m above the river bed) show significant discrepancies between carbonate and organic fractions. The organic residue dates (20–8 cal kBP) implies tufa deposition mainly during the MIS 2 period and partially in the early Holocene. Radiocarbon dates obtained from the carbonate fraction (42–25 cal kBP) indicate mostly MIS 3 deposition. The carbonate ages are argued to be more reliable since tufa deposition principally during MIS 3 is supported by the oxygen isotopic composition of the carbonate fraction. Organic-fraction dates are rejected since tufa deposition during the deep glacial of MIS 2 is highly unlikely. Additionally, humin dates indicate contamination of the organic fraction of tufa with younger plant-sourced  $^{14}\text{C}$ , as dates obtained from humin residues were younger than bulk organic residues, especially in the case of older tufa deposits. Finally, radiocarbon dates of the carbonate fraction of 20–40 kyr confirm previous estimates that the palaeo-Zrmanja River course differed from its current position (led probably into the Krka River) and that the new part of the Zrmanja river bed developed after 40 kBP, with a major incision period between 25,000 and 6000 cal BP, and an estimated incision rate of 1.1 mm/yr.

This research opens numerous possibilities for further investigation along the Zrmanja River and contributes to the understanding of regional paleoenvironmental changes.

**Supplementary Materials:** The following are available online at <https://www.mdpi.com/article/10.3390/geosciences11090376/s1>, Figure S1: Characteristic tufa samples from the Zrmanja River Canyon.

**Author Contributions:** Conceptualization, J.B., S.F. and I.K.B.; methodology, J.B., A.S., R.N.D. and D.B.; formal analysis, J.B.; investigation, J.B. and S.F.; resources, I.K.B.; data curation, J.B., A.S., I.L.M. and D.B.; writing—original draft preparation, J.B.; writing—review and editing, J.B., I.K.B., S.F., R.N.D. and A.S.; visualization, J.B., I.K.B. and I.L.M.; project administration, I.K.B. All authors have read and agreed to the published version of the manuscript.

**Funding:** This research was funded by Croatian Science Foundation grant number HRZZ-IP-2013-11-1623 (Reconstruction of the Quaternary environment in Croatia using isotope methods—REQUENCRIM).

**Institutional Review Board Statement:** Not applicable.

**Informed Consent Statement:** Not applicable.

**Data Availability Statement:** All relevant data are presented in this paper.

**Acknowledgments:** The authors thank Janislav Kapelj, Maša Surić, Robert Lončarić, and Dražen Perica for help in sampling. The authors thank Nada Horvatinčić for continuous interest and help in the research of karst phenomena.

**Conflicts of Interest:** The authors declare no conflict of interest. The funders had no role in the design of the study; in the collection, analyses, or interpretation of data; in the writing of the manuscript, or in the decision to publish the results.

## References

1. Ford, T.D.; Pedley, H.M. A review of tufa and travertine deposits of the world. *Earth-Science Rev.* **1996**, *41*, 117–175. [[CrossRef](#)]
2. Gandin, A.; Capezzuoli, E. Travertine versus calcareous tufa: Distinctive petrologic features and stable isotopes signatures. *Quaternario* **2008**, *21*, 125–136.
3. Capezzuoli, E.; Gandin, A.; Pedley, M. Decoding tufa and travertine (fresh water carbonates) in the sedimentary record: The state of the art. *Sedimentology* **2013**, *61*, 1–21. [[CrossRef](#)]
4. Horvatinčić, N.; Krajcar Bronić, I.; Obelić, B. Differences in the  $^{14}\text{C}$  age,  $\delta^{13}\text{C}$  and  $\delta^{18}\text{O}$  of Holocene tufa and speleothem in the Dinaric Karst. *Palaeogeogr. Palaeoclim. Palaeoecol.* **2003**, *193*, 139–157. [[CrossRef](#)]
5. Srdoč, D.; Obelić, B.; Horvatinčić, N. Radiocarbon dating of calcareous tufa: How reliable data can we expect? *Radiocarbon* **1980**, *22*, 858–862. [[CrossRef](#)]
6. Brook, G.A.; Railsback, L.B.; Marais, E. Reassessment of carbonate ages by dating both carbonate and organic material from an Etosha Pan (Namibia) stromatolite: Evidence of humid phases during the last 20ka. *Quat. Int.* **2011**, *229*, 24–37. [[CrossRef](#)]
7. Brook, G.A.; Cherkinsky, A.; Railsback, L.B.; Marais, E.; Hipondoka, M.H.T.  $^{14}\text{C}$  dating of organic residue and carbonate from stromatolites in Etosha Pan, Namibia:  $^{14}\text{C}$  reservoir effect: Correction of published ages and evidence of >8-m-deep lake during the late Pleistocene. *Radiocarbon* **2013**, *55*, 1156–1163. [[CrossRef](#)]
8. Blyth, A.J.; Hua, Q.; Smith, A.; Frisia, S.; Borsato, A.; Hellstrom, J. Exploring the dating of “dirty” speleothems and cave sinters using radiocarbon dating of preserved organic matter. *Quat. Geochronol.* **2017**, *39*, 92–98. [[CrossRef](#)]
9. Andrews, J. Palaeoclimatic records from stable isotopes in riverine tufas: Synthesis and review. *Earth-Sci. Rev.* **2006**, *75*, 85–104. [[CrossRef](#)]
10. Rainey, D.K.; Jones, B. Rapid cold water formation and recrystallization of relict bryophyte tufa at the Fall Creek cold springs, Alberta, Canada. *Can. J. Earth Sci.* **2007**, *44*, 889–909. [[CrossRef](#)]
11. Horvatinčić, N.; Čalić, R.; Geyh, M.A. Interglacial Growth of Tufa in Croatia. *Quat. Res.* **2000**, *53*, 185–195. [[CrossRef](#)]
12. Pentecost, A. *Travertine*; Springer: Berlin/Heidelberg, Germany, 2005; p. 445.
13. Pazdur, A.; Goslar, T.; Pawlyta, M.; Hercman, H.; Gradziński, M. Variations of Isotopic Composition of Carbon in the Karst Environment from Southern Poland, Present and Past. *Radiocarbon* **1999**, *41*, 81–97. [[CrossRef](#)]
14. Andrews, J.E.; Riding, R.; Dennis, P. The stable isotope record of environmental and climatic signals in modern terrestrial microbial carbonates from Europe. *Palaeogeogr. Palaeoclim. Palaeoecol.* **1997**, *129*, 171–189. [[CrossRef](#)]
15. Pedley, M. Tufas and travertines of the Mediterranean region: A testing ground for freshwater carbonate concepts and developments. *Sedimentology* **2009**, *56*, 221–246. [[CrossRef](#)]
16. Vazquez-Urbez, M.; Pardo, G.; Arenas, C.; Sancho, C. Fluvial diffluence episodes reflected in the Pleistocene tufa deposits of the River Piedra (Iberian Range, NE Spain). *Geomorphology* **2011**, *125*, 1–10. [[CrossRef](#)]
17. Domínguez-Villar, D.; Vázquez-Navarro, J.A.; Cheng, H.; Edwards, R.L. Freshwater tufa record from Spain supports evidence for the past interglacial being wetter than the Holocene in the Mediterranean region. *Glob. Planet. Chang.* **2011**, *77*, 129–141. [[CrossRef](#)]
18. Valero-Garcés, B.; Morellón, M.; Moreno, A.; Corella, J.P.; Martín-Puertas, C.; Barreiro, F.; Pérez, A.; Giral, S.; Mata-Campo, M.P. Lacustrine carbonates of Iberian Karst Lakes: Sources, processes and depositional environments. *Sediment. Geol.* **2014**, *299*, 1–29. [[CrossRef](#)]
19. Dabkowski, J. The late-Holocene tufa decline in Europe: Myth or reality? *Quat. Sci. Rev.* **2020**, *230*, 106141. [[CrossRef](#)]
20. Suchý, V.; Zachariáš, J.; Tsai, H.-C.; Yu, T.-L.; Shen, C.-C.; Svetlik, I.; Havelcová, M.; Borecká, L.; Machovič, V. Relict Pleistocene calcareous tufa of the Chlupáčova sluj Cave, the Bohemian Karst, Czech Republic: A petrographic and geochemical record of hydrologically-driven cave evolution. *Sediment. Geol.* **2019**, *385*, 110–125. [[CrossRef](#)]
21. Drysdale, R.; Head, J. Geomorphology, Stratigraphy and  $^{14}\text{C}$ -Chronology of Ancient Tufas at Louie Creek, Northwest Queensland, Australia. *Géographie Phys. Quat.* **1994**, *48*, 285–295. [[CrossRef](#)]
22. Alexandrowicz, W.P.; Szymanek, M.; Rybska, E. Changes to the environment of intramontane basins in the light of malacological research of calcareous tufa: Podhale Basin (Carpathians, Southern Poland). *Quat. Int.* **2014**, *353*, 250–265. [[CrossRef](#)]
23. Sherriff, J.E.; Schreve, D.C.; Candy, I.; Palmer, A.P.; White, T.S. Environments of the climatic optimum of MIS 11 in Britain: Evidence from the tufa sequence at Hitchin, southeast England. *J. Quat. Sci.* **2021**, *36*, 508–525. [[CrossRef](#)]
24. Hasan, O.; Miko, S.; Brunović, D.; Papatheodorou, G.; Christodolou, D.; Ilijanić, N.; Geraga, M. Geomorphology of Canyon Outlets in Zrmanja River Estuary and Its Effect on the Holocene Flooding of Semi-enclosed Basins (the Novigrad and Karin Seas, Eastern Adriatic). *Water* **2020**, *12*, 2807. [[CrossRef](#)]
25. Marić, I.; Šiljeg, A.; Cukrov, N.; Roland, V.; Domazetović, F. How fast does tufa grow? Very high-resolution measurement of the tufa growth rate on artificial substrates by the development of a contactless image-based modelling device. *Earth Surf. Process. Landf.* **2020**, *45*, 2331–2349. [[CrossRef](#)]
26. Krajcar Bronić, I.; Barešić, J.; Sironić, A. Application of  $^{14}\text{C}$  method to chronology of the Croatian Dinaric karst—A case of the Plitvice Lakes. *Radiocarbon* **2021**, 1–13, (online first). [[CrossRef](#)]

27. Deevey, E.S.; Gross, M.S.; Hutchinson, G.E.; Kraybill, H.L. The Natural C14 Contents of materials from hard-water lakes. *Proc. Natl. Acad. Sci. USA* **1954**, *40*, 285–288. [[CrossRef](#)] [[PubMed](#)]
28. Faivre, S.; Bakran-Petricioli, T.; Barešić, J.; Horvatinčić, N. New data on the marine radiocarbon reservoir effect in the Eastern Adriatic based on pre-bomb marine organisms from the intertidal zone and shallow sea. *Radiocarbon* **2015**, *57*, 527–538. [[CrossRef](#)]
29. Faivre, S.; Bakran-Petricioli, T.; Barešić, J.; Morhange, C.; Borković, D. Marine radiocarbon reservoir age of the coralline inter-tidal alga *Lithophyllum byssoides* in the Mediterranean. *Quat. Geochronol.* **2019**, *51*, 15–23. [[CrossRef](#)]
30. Stuiver, M.; Pearson, G.W.; Braziunas, T. Radiocarbon Age Calibration of Marine Samples Back to 9000 Cal Yr BP. *Radiocarbon* **1986**, *28*, 980–1021. [[CrossRef](#)]
31. Genty, D.; Massault, M.; Gilmour, M.; Baker, A.; Verheyden, S.; Kepens, E. Calculation of Past Dead Carbon Proportion and Variability by the Comparison of AMS 14C and Tims U/TH Ages on Two Holocene Stalagmites. *Radiocarbon* **1999**, *41*, 251–270. [[CrossRef](#)]
32. Bajo, P.; Borsato, A.; Drysdale, R.; Hua, Q.; Frisia, S.; Zanchetta, G.; Hellstrom, J.; Woodhead, J. Stalagmite carbon isotopes and dead carbon proportion (DCP) in a near-closed-system situation: An interplay between sulphuric and carbonic acid dissolution. *Geochim. Cosmochim. Acta* **2017**, *210*, 208–227. [[CrossRef](#)]
33. Dabkowski, J. High potential of calcareous tufas for integrative multidisciplinary studies and prospects for archaeology in Europe. *J. Archaeol. Sci.* **2014**, *52*, 72–83. [[CrossRef](#)]
34. Horvatinčić, N.; Barešić, J.; Babinka, S.; Obelić, B.; Krajcar Bronić, I.; Vreča, P.; Suckow, A. Towards a deeper understanding how carbonate isotopes (14C, 13C, 18O) reflect environmental changes: A study with recent 210Pb dated sediments of the Plitvice lakes, Croatia. *Radiocarbon* **2008**, *50*, 233–253. [[CrossRef](#)]
35. Zagorevski, A.; Rogers, N.; Van Staal, C.; McNicoll, V.; Lissenberg, J.; Valverde-Vaquero, P. Lower to Middle Ordovician evolution of peri-Laurentian arc and backarc complexes in Iapetus: Constraints from the Annieopsquotch accretionary tract, central Newfoundland. *GSA Bull.* **2006**, *118*, 324–342. [[CrossRef](#)]
36. Luo, S.; Ku, T.-L. U-series isochron dating: A generalized method employing total-sample dissolution. *Geochim. Cosmochim. Acta* **1991**, *55*, 555–564. [[CrossRef](#)]
37. Hellstrom, J. U–Th dating of speleothems with high initial 230Th using stratigraphical constraint. *Quat. Geochronol.* **2006**, *1*, 289–295. [[CrossRef](#)]
38. Brasier, A.T.; Andrews, J.E.; Marca-Bell, A.D.; Dennis, P.F. Depositional continuity of seasonally laminated tufas: Implications for  $\delta^{18}O$  based palaeotemperatures. *Glob. Planet. Chang.* **2010**, *71*, 160–167. [[CrossRef](#)]
39. Hamdan, M.A.; Brook, G.A. Timing and characteristics of Late Pleistocene and Holocene wetter periods in the Eastern Desert and Sinai of Egypt, based on 14C dating and stable isotope analysis of spring tufa deposits. *Quat. Sci. Rev.* **2015**, *130*, 168–188. [[CrossRef](#)]
40. Wang, Z.; Zhao, H.; Dong, G.; Zhou, A.; Liu, J.; Zhang, D. Reliability of radiocarbon dating on various fractions of loess-soil sequence for Dadiwan section in the western Chinese Loess Plateau. *Front. Earth Sci.* **2014**, *8*, 540–546. [[CrossRef](#)]
41. Pessenda, L.C.R.; Gouveia, S.E.M.; Aravena, R. Radiocarbon Dating of Total Soil Organic Matter and Humic Fraction and Its Comparison with 14C Ages of Fossil Charcoal. *Radiocarbon* **2001**, *43*, 595–601. [[CrossRef](#)]
42. Balesdent, J. The turnover of soil organic fractions estimated by radiocarbon dating. *Sci. Total Environ.* **1987**, *62*, 405–408. [[CrossRef](#)]
43. Balesdent, J.; Guillet, B. Les datations par le 14C des matières organiques des sols. Contribution à l'étude de l'humification et du renouvellement des substances humiques. *Sci. Sol.* **1992**, *2*, 93–112.
44. Becker-Heidmann, P.; Liang-Wu, L.; Scharpenseel, H.-W. Radiocarbon Dating of Organic Matter Fractions of a Chinese Mollisol. *J. Plant Nutr. Soil Sci.* **1988**, *151*, 37–39. [[CrossRef](#)]
45. Veveřec, I. Sedra na rijeci Zrmanji kao nedovoljno istraženi i valorizirani geomorfološki fenomen. *Acta Geogr. Croat.* **2019**, *45–46*, 69–83.
46. Pavlek, K.; Faivre, S. Geomorphological changes of the Cetina River channels since the end of the nineteenth century, natural vs anthropogenic impacts (the Dinarides, Croatia). *Environ. Earth Sci.* **2020**, *79*, 1–16. [[CrossRef](#)]
47. Fritz, F. Razvitak gornjeg toka rijeke Zrmanje. *Carsus Jugosl.* **1972**, *8*, 1–16. (In Croatian)
48. Kapelj, J.; Fritz, F. *Bojenje ponora uz Rijeku Zrmanju u Erveničkom Polju*; Arhiv HGI: Zagreb, Croatia, 1986.
49. Bonacci, O. Water circulation in karst and determination of catchment areas: Example of the River Zrmanja. *Hydrol. Sci. J.* **1999**, *44*, 373–386. [[CrossRef](#)]
50. Pavlović, G.; Prohić, E.; Miko, S.; Tibljaš, D. Geochemical and petrographic evidence of meteoric diagenesis in tufa deposits in Northern Dalmatia (Zrmanja and Krupa Rivers, Croatia). *Facies* **2002**, *46*, 27–34. [[CrossRef](#)]
51. Croatian Geological Survey. *Geological Map of Republic of Croatia, M 1:300 000*; Croatian Geological Survey: Zagreb, Croatia, 1999. (In Croatian)
52. Horvatinčić, N.; Barešić, J.; Krajcar Bronić, I.; Obelić, B. Measurement of low 14C activities in a liquid scintillation counter in the Zagreb Radiocarbon Laboratory. *Radiocarbon* **2004**, *46*, 105–116. [[CrossRef](#)]
53. Krajcar Bronić, I.; Horvatinčić, N.; Barešić, J.; Obelić, B. Measurement of 14C activity by liquid scintillation counting. *Appl. Radiat. Isot.* **2009**, *67*, 800–804. [[CrossRef](#)]
54. Sironić, A.; Krajcar Bronić, I.; Horvatinčić, N.; Barešić, J.; Obelić, B.; Felja, I. Status report on the Zagreb Radiocarbon Laboratory—AMS and LSC results of VIRI intercomparison samples. *Nucl. Instrum. Methods B* **2013**, *294*, 185–188. [[CrossRef](#)]

55. Brock, F.; Higham, T.; Ditchfield, P.; Ramsey, C.B. Current Pretreatment Methods for AMS Radiocarbon Dating at the Oxford Radiocarbon Accelerator Unit (Orau). *Radiocarbon* **2010**, *52*, 103–112. [CrossRef]
56. Dunbar, E.; Cook, G.T.; Naysmith, P.; Tripney, B.; Xu, S. AMS 14C Dating at the Scottish Universities Environmental Research Centre (SUERC) Radiocarbon Dating Laboratory. *Radiocarbon* **2016**, *58*, 9–23. [CrossRef]
57. Cherkinsky, A.E.; Culp, R.A.; Dvoracek, D.K.; Noakes, J.E. Status of the AMS facility at the Center for Applied Isotope Studies, University of Georgia. *Nucl. Instrum. Methods B* **2010**, *268*, 867–870. [CrossRef]
58. Ramsey, C.B. Bayesian Analysis of Radiocarbon Dates. *Radiocarbon* **2009**, *51*, 337–360. [CrossRef]
59. Ramsey, B.C. OxCal v.4.4.4. 2021. Available online: <https://c14.arch.ox.ac.uk/oxcal/OxCal.html> (accessed on 22 March 2021).
60. Reimer, P.J.; Austin, W.E.N.; Bard, E.; Bayliss, A.; Blackwell, P.G.; Ramsey, C.B.; Butzin, M.; Cheng, H.; Edwards, R.L.; Friedrich, M.; et al. The intcal20 northern hemisphere radiocarbon age calibration curve (0–55 CAL kBP). *Radiocarbon* **2020**, *62*, 725–757. [CrossRef]
61. Drysdale, R.N.; Hellstrom, J.C.; Zanchetta, G.; Fallick, A.E.; Goni, M.F.S.; Couchoud, I.; McDonald, J.; Maas, R.; Lohmann, G.; Isola, I. Evidence for Obliquity Forcing of Glacial Termination II. *Science* **2009**, *325*, 1527–1531. [CrossRef]
62. Sironić, A.; Alegro, A.; Horvatinčić, N.; Barešić, J.; Brozinčević, A.; Vurnek, M.; Krajcar Bronić, I.; Borković, D.; Lovrenčić Mikelić, I. Carbon isotope fractionation in karst aquatic mosses. *Isot. Environ. Health Stud.* **2020**, *57*, 142–165. [CrossRef]
63. Horvatinčić, N.; Sironić, A.; Barešić, J.; Sondi, I.; Krajcar Bronić, I.; Borković, D. Mineralogical, organic and isotopic composition as palaeoenvironmental records in the lake sediments of two lakes, the Plitvice Lakes, Croatia. *Quat. Int.* **2018**, *494*, 300–313. [CrossRef]
64. Horvatinčić, N.; Krajcar Bronić, I.; Obelić, B.; Barešić, J. Rudjer Bošković Institute radiocarbon measurements XVII. *Radiocarbon* **2012**, *54*, 137–154. [CrossRef]
65. Hays, P.D.; Grossman, E.L. Oxygen isotopes in meteoric calcite cements as indicators of continental palaeoclimate. *Geology* **1991**, *19*, 441–444. [CrossRef]
66. Lojen, S.; Dolenc, T.; Vokal, B.; Cukrov, N.; Mihelčić, G.; Papesch, W. C and O stable isotope variability in recent freshwater carbonates (River Krka, Croatia). *Sedimentology* **2004**, *51*, 361–375. [CrossRef]
67. Lojen, S.; Dolenc, M.; Cukrov, N. Palaeothermometry in tufa: A case study from the Krka National Park, Croatia. *RMZ—Mater. Geoenviron.* **2014**, *61*, 87–96.
68. Terzić, J.; Marković, T.; Reberski, J.L. Hydrogeological properties of a complex Dinaric karst catchment: Miljacka Spring case study. *Environ. Earth Sci.* **2014**, *72*, 1129–1142. [CrossRef]
69. Cukrov, N.; Tepić, N.; Omanović, D.; Lojen, S.; Bura Nakić, E.; Vojvodić, V.; Pižeta, I. Qualitative interpretation of physico-chemical and isotopic parameters in the Krka River (Croatia) assessed by multivariate statistical analysis. *Int. J. Env. Anal. Chem.* **2012**, *92*, 1187–1199. [CrossRef]
70. Pavlova, E.Y.; Pitulko, V.V. Late Pleistocene and Early Holocene climate changes and human habitation in the arctic Western Beringia based on revision of palaeobotanical data. *Quat. Int.* **2020**, *549*, 5–25. [CrossRef]
71. Loftus, E.; Stewart, B.; Dewar, G.; Leethorp, J. Stable isotope evidence of late MIS 3 to middle Holocene palaeoenvironments from Sehonghong Rockshelter, eastern Lesotho. *J. Quat. Sci.* **2015**, *30*, 805–816. [CrossRef]
72. Petit, J.R.; Jouzel, J.; Raynaud, D.; Barkov, N.I.; Barnola, J.-M.; Basile-Doelsch, I.; Bender, M.L.; Chappellaz, J.; Davis, M.L.; Delaygue, G.; et al. Climate and atmospheric history of the past 420,000 years from the Vostok ice core, Antarctica. *Nature* **1999**, *399*, 429–436. [CrossRef]
73. Srdoč, D.; Obelić, B.; Horvatinčić, N.; Krajcar Bronić, I.; Marčenko, E.; Merkt, S.; Wong, H.; Sliepčević, A. Radiocarbon dating of lake sediments from two Karstic lakes in Yugoslavia. *Radiocarbon* **1986**, *28*, 495–502. [CrossRef]
74. Krajcar Bronić, I.; Barešić, J.; Sironić, A.; Lovrenčić Mikelić, I.; Borković, D.; Horvatinčić, N.; Kovač, Z. Isotope Composition of Precipitation, Groundwater, and Surface and Lake Waters from the Plitvice Lakes, Croatia. *Water* **2020**, *12*, 2414. [CrossRef]
75. Tanner, L.H. Chapter 4 Continental Carbonates as Indicators of Paleoclimate. In *Developments in Sedimentology*; Alonso-Zarza, A.M., Tanner, L.H., Eds.; Elsevier: Amsterdam, The Netherlands, 2010; Volume 62, pp. 179–214. [CrossRef]
76. Vreča, P.; Krajcar Bronić, I.; Horvatinčić, N.; Barešić, J. Isotopic characteristics of precipitation in Slovenia and Croatia: Comparison of continental and maritime stations. *J. Hydrol.* **2006**, *330*, 457–469. [CrossRef]
77. Gonfiantini, R.; Roche, M.-A.; Olivry, J.-C.; Fontes, J.-C.; Zuppi, G.M. The altitude effect on the isotopic composition of tropical rains. *Chem. Geol.* **2001**, *181*, 147–167. [CrossRef]
78. Rozanski, K.; Araguás-Araguás, L.; Gonfiantini, R. Isotopic Patterns in Modern Global Precipitation. *Geophys. Monogr.* **1993**, *78*, 1–36.
79. Peel, M.C.; Finlayson, B.L.; McMahon, T.A. Updated world map of the Köppen-Geiger climate classification. *Hydrol. Earth Syst. Sci.* **2007**, *11*, 1633–1644. [CrossRef]
80. Filipčić, A. Climatic Regionalization of Croatia According to W. Koeppen for the Standard Period 1961–1990 in Relation to the Period 1931–1960. *Acta Geogr. Croat.* **1998**, *33*, 7–15.
81. Köppen, W. Das geographische System der Klimate. In *Handbuch der Klimatologie*; Köppen, W., Geiger, G., Eds.; Gebrüder Borntraeger: Berlin, Germany, 1936; pp. 1–44.
82. Vogel, J.S.; Southon, J.R.; Nelson, D.E.; Brown, T.A. Performance of catalytically condensed carbon for use in accelerator mass spectrometry. *Nucl. Instrum. Methods Phys. Res. Sect. B* **1984**, *5*, 289–293. [CrossRef]
83. Horvatinčić, N.; Sironić, A.; Barešić, J.; Krajcar Bronić, I.; Todorović, N.; Nikolov, J.; Hansman, J.; Krmar, M. Isotope analyses of the lake sediments in the Plitvice Lakes, Croatia. *Cent. Eur. J. Phys.* **2014**, *12*, 707–713. [CrossRef]

84. Marčenko, E.; Srdoč, D.; Golubić, S.; Pezdič, J.; Head, M.J. Carbon Uptake in Aquatic Plants Deduced From Their Natural  $^{13}\text{C}$  and  $^{14}\text{C}$  Content. *Radiocarbon* **1989**, *31*, 785–794. [[CrossRef](#)]
85. Hodell, D.; Schelske, C.L. Production, sedimentation, and isotopic composition of organic matter in Lake Ontario. *Limnol. Oceanogr.* **1998**, *43*, 200–214. [[CrossRef](#)]
86. Meyers, P.A. Applications of organic geochemistry to paleolimnological reconstructions: A summary of examples from the Laurentian Great Lakes. *Org. Geochem.* **2003**, *34*, 261–289. [[CrossRef](#)]
87. Francey, R.J.; Allison, C.E.; Etheridge, D.M.; Trudinger, C.; Enting, I.; Leuenberger, M.C.; Langenfelds, R.L.; Michel, E.; Steele, L.P. A 1000-year high precision record of  $\delta^{13}\text{C}$  in atmospheric  $\text{CO}_2$ . *Tellus B Chem. Phys. Meteorol.* **1999**, *51*, 170–193. [[CrossRef](#)]
88. Hammer, S.; Levin, I. *Monthly mean atmospheric  $\Delta^{14}\text{CO}_2$  at Jungfraujoch and Schauinsland from 1986 to 2016*; Heidelberg University—Institute of Environmental Physics: Heidelberg, Germany, 2017. [[CrossRef](#)]
89. Borković, D.; Krajcar Bronić, I.; Sironić, A.; Barešić, J. Comparison of sampling and measurement methods for atmospheric  $^{14}\text{C}$  activity. In: Book of Abstracts. In Proceedings of the 9th International Conference on Radiation in Various fields of Research—RAD2021, Herceg Novi, Montenegro, 14–18 June 2021; p. 266.
90. Hua, Q.; Barbetti, M.; Rakowski, A. Atmospheric Radiocarbon for the Period 1950–2010. *Radiocarbon* **2013**, *55*, 2059–2072. [[CrossRef](#)]
91. Cheng, H.; Edwards, R.L.; Southon, J.; Matsumoto, K.; Feinberg, J.M.; Sinha, A.; Zhou, W.; Li, H.; Li, X.; Xu, Y.; et al. Atmospheric  $^{14}\text{C}/^{12}\text{C}$  changes during the last glacial period from Hulu Cave. *Science* **2018**, *362*, 1293–1297. [[CrossRef](#)]
92. Cheng, H.; Zhang, H.; Spötl, C.; Baker, J.; Sinha, A.; Li, H.; Bartolomé, M.; Moreno, A.; Kathayat, G.; Zhao, J.; et al. Timing and structure of the Younger Dryas event and its underlying climate dynamics. *Proc. Natl. Acad. Sci. USA* **2020**, *117*, 23408–23417. [[CrossRef](#)] [[PubMed](#)]
93. Hemming, S. Heinrich events: Massive late Pleistocene detritus layers of the North Atlantic and their global climate imprint. *Rev. Geophys.* **2004**, *42*, RG1005. [[CrossRef](#)]
94. Lisiecki, L.E.; Raymo, M.E. A Pliocene-Pleistocene stack of 57 globally distributed benthic  $\delta^{18}\text{O}$  records. *Paleoceanography* **2005**, *20*. [[CrossRef](#)]
95. Srdoč, D.; Horvatinčić, N.; Obelić, B.; Krajcar Bronić, I.; Sliepčević, A. Procesi taloženja kalcita u krškim vodama s posebnim osvrtom na Plitvička jezera (Calcite deposition processes in karstwaters with special emphasis on the Plitvice Lakes, Yugoslavia). *Carsus Jugosl.* **1985**, *11*, 101–204.
96. Belij, S. Komparativnost krškog, glacialnog i periglacialnog procesa u reljefu Južnog Velebita [Comparison of karst, glacial and periglacial process in the relief of southern Velebit—In Croatian]. *Acta Carsologica* **1986**, *14–15*, 183–196.
97. Bognar, A.; Faivre, S.; Pavelić, J. Tragovi oledbe na Sjevernom Velebitu [Glaciation traces on the Northern Velebit]. *Geogr. Glas.* **1991**, *53*, 27–39.
98. Bognar, A.; Faivre, S. Geomorphological traces of the younger Pleistocene glaciation in the central part of the Velebit Mt. *Hrvat. Geogr. Glas.* **2006**, *68*, 19–30. [[CrossRef](#)]
99. Bočić, N.; Faivre, S.; Kovačić, M.; Horvatinčić, N. Cave development under the influence of Pleistocene glaciation in the Dinarides—An example from Štirovača ice cave (Velebit Mt., Croatia). *Z. Geomorph. NF* **2012**, *56*, 409–433. [[CrossRef](#)]
100. Surić, M.; Juračić, M. Late Pleistocene-Holocene environmental changes—Records from submerged speleothems along the Eastern Adriatic coast (Croatia). *Geol. Croat.* **2010**, *63*, 155–169. [[CrossRef](#)]
101. Lončar, N. Isotopic Composition of the Speleothems from the Eastern Adriatic Islands Caves as an Indicator of Palaeoenvironmental Changes. Ph.D. Thesis, Faculty of Science, University of Zagreb, Zagreb, Croatia, 2012.
102. Surić, M.; Lončarić, R.; Columbu, A.; Bajo, P.; Lončar, N.; Drysdale, R.; Hellstrom, J. Environmental change in the Adriatic region over the last 365 kyr from episodic deposition of Modrič Cave (Croatia) speleothems. In Proceedings of the 20th INQUA Congress, Dublin, Ireland, 25–31 July 2019.
103. Fairbanks, R.G. A 17,000-year glacio-eustatic sea level record: Influence of glacial melting rates on the Younger Dryas event and deep-ocean circulation. *Nature* **1989**, *342*, 637–642. [[CrossRef](#)]
104. Correggiari, A.; Roveri, M.; Trincardi, F. Late Pleistocene and Holocene evolution of the North Adriatic Sea. *Quaternario* **1996**, *9*, 697–704.
105. Lambeck, K.; Esat, T.; Potter, E.-K. Links between climate and sea levels for the past three million years. *Nature* **2002**, *419*, 199–206. [[CrossRef](#)] [[PubMed](#)]
106. Lambeck, K.; Yokoyama, Y.; Purcell, A. Into and out of the Last Glacial Maximum: Sea-level change during Oxygen Isotope Stages 3 and 2. *Quat. Sci. Rev.* **2002**, *21*, 343–360. [[CrossRef](#)]
107. Waelbroeck, C.; Labeyrie, L.; Michel, E.; Duplessy, J.; McManus, J.; Lambeck, K.; Balbon, E.; Labracherie, M. Sea-level and deep water temperature changes derived from benthic foraminifera isotopic records. *Quat. Sci. Rev.* **2002**, *21*, 295–305. [[CrossRef](#)]
108. Antonioli, F.; Furlani, S.; Montagna, P.; Stocchi, P. The Use of Submerged Speleothems for Sea Level Studies in the Mediterranean Sea: A New Perspective Using Glacial Isostatic Adjustment (GIA). *Geosciences* **2021**, *11*, 77. [[CrossRef](#)]
109. Ortiz, J.; Torres, T.; Delgado, A.; Reyes, E.; Díaz-Bautista, A. A review of the Tagus river tufa deposits (central Spain): Age and palaeoenvironmental record. *Quat. Sci. Rev.* **2009**, *28*, 947–963. [[CrossRef](#)]
110. Ollivier, V.; Guendon, J.-L.; Ali, A.; Roiron, P.; Ambert, P. Évolution postglaciaire des environnements travertineux provençaux et alpins: Nouveau cadre chronologique, faciès et dynamiques morphosédimentaires. *Quaternaire* **2006**, *17*, 51–67. [[CrossRef](#)]